AIP Publishing

This manuscript was accepted by Appl. Phys. Lett. Click here to see the version of record.

The role of bandgap energy excess in surface emission of terahertz radiation from semiconductors

M. Alfaro-Gomez
Departamento de Matematicas y Fisica,
Universidad Autonoma de Aguascalientes,
Av. Universidad 940, Ciudad Universitaria,
C.P. 20131, Aguascalientes, Mexico

E. Castro-Camus*
Centro de Investigaciones en Optica A.C.,
Loma del Bosque 115, Lomas del Campestre,
C.P. 37150 Leon, Guanajuato, Mexico

(Dated: December 22, 2016)

We use a Monte-Carlo model to simulate semi-classical photo-carrier dynamics of InAs, InGaAs and GaAs that leads to terahertz emission. We compare the emission power of all three semiconductors as function of excitation photon energy finding that the carrier excess excitation energy is more relevant to explain their performance difference than their mobilities. We conclude that ballistic transport after photoexcitation is the dominant mechanism for terahertz emission instead of diffusion driven or surface field driven charge separation, which were traditionally considered the most relevant mechanisms.

PACS numbers: 78.47.-p, 78.47.J-, 78.47.D-, 73.23.Ad

ACCEPTED MANUSCRIPT

Terahertz emission from semiconductor surfaces after ultrafast photoexcitation has been the subject of intensive research [1–5]. This phenomenon is relevant not only because it is a useful tool for the production of terahertz radiation [6, 7], but also because it has helped to reveal aspects of the carrier dynamics in such materials [8–10]. Broadly speaking, two main mechanisms for emission have been identified. Firstly, the material's electric field produced by the band pining near the surface is expected to generate charge acceleration perpendicular to the semiconductor's surface, this is thought to be the dominant mechanism in broad bandgap materials such as GaAs [9, 11, 12]. In contrast, the large difference of electron and hole mobilities in narrow bandgap semiconductors is thought to be the reason for diffusion driven charge separation in materials such as InAs [11, 13, 14], in the direction normal to the surface as well. This last phenomenon is known as the photo-Dember effect. Some recent studies have observed the emission of terahertz from semiconductor surfaces in the near field [15, 16] and in combination with simulations have demonstrated that transient photocurrents in the direction parallel to the surface are also relevant in the terahertz emission process [17]. In this letter, we report simulations that demonstrate that the initial kinetic energy of carriers owing to the pump photon bandgap excess energy determines to a good extent the emitted terahertz power, and that ballistic transport owing to this excess energy is the dominant mechanism for terahertz emission. This theory explains much better the difference in laser-to-power conversion efficiency between InAs, InGaAs and GaAs at 800 nm and represents a change in paradigm of the physics behind terahertz emission.

The carrier dynamics of GaAs, $In_{0.53}Ga_{0.47}As$ (InGaAs) and InAs was simulated under ultrafast photoexcitation using a semiclassical Monte Carlo approach. A volume of $35\,\mu\text{m}\times 35\,\mu\text{m}\times 10\,\mu\text{m}$ was simulated using the computational code described in [8, 11, 17, 18]. The simulation volume is divided into a $120 \times 120 \times 40$ partition mesh. One million pseudo-particles are used to simulate intrinsic and photogenerated carriers move within this three-dimensional space. They are assumed to move classically in 1 fs time steps. Initially, a random distribution of intrinsic carriers with energies given by a Maxwell-Boltzman distribution is assumed. The charge density across the partition is calculated; from it, the Poisson equation is solved and the electric field is calculated which in turn is used to calculate the force acting on each carrier in the next time step. The potential at the surface boundary of the semiconductor is fixed to the pinning potential $\Phi(x, y, z = 0) = \Phi_s$ and a Neumann boundary condition where used for the rest of the boundaries. After 1.5 ps a normal incidence optical pulse of Gaussian temporal and spatial profile (τ=100 fs, $\sigma_{\text{x,y}}$=5 μm) excites the semiconductor injecting additional carriers to the simulation. For each time step, we calculate carrier scattering rates for LO-phonons, TO-phonon mediated intervalley (Γ, L and X), acoustic phonons, charged impurity and carrier-carrier interactions. Pseudo-random numbers are used to decide if each carrier scatters, and to determine its scattering angle and energy change. We perform simulations without carrier-carrier scattering finding marginal differences with the ones including

* enrique@cio.mx; http://www.thz.org.mx

AIP Publishing

This manuscript was accepted by Appl. Phys. Lett. Click here to see the version of record.

ACCEPTED MANUSCRIPT

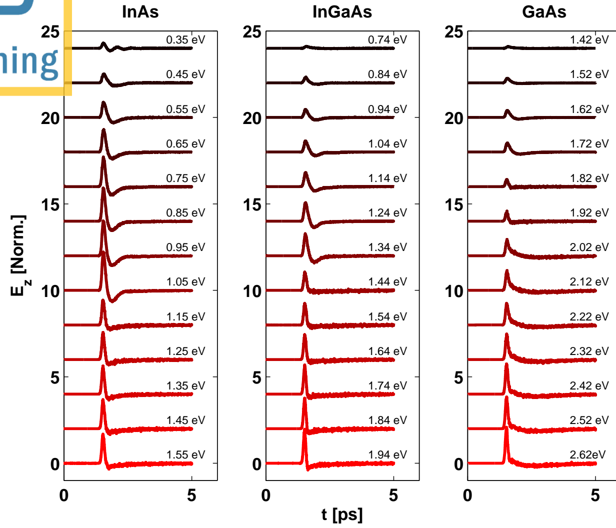

FIG. 1. Simulated THz electric field emitted at various photon excitation energies. Each set is normalized and an offset has been added for visualization.

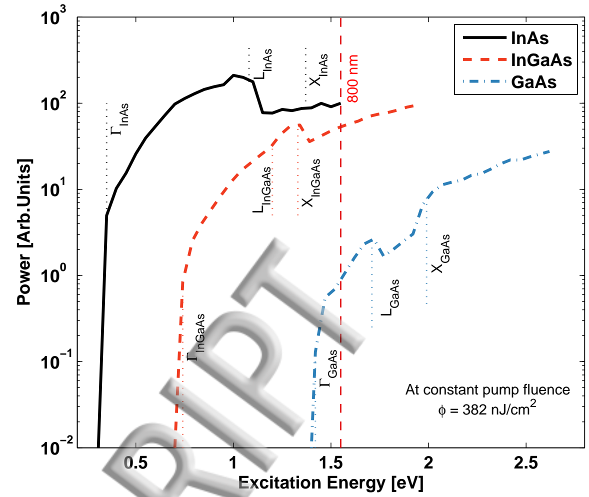

FIG. 2. Emission power as a function of excitation energy at a pump fluence of 382 nJ/cm^2. Γ, L and X valleys for each material are marked. 800 nm energy is indicated by vertical dashed line.

TABLE I. Semiconductor parameters used in the simulation.

	InAs	InGaAs	GaAs
Γ valley effective mass, $m*_\Gamma$	$0.022m_0$	$0.04m_0$	$0.067m_0$
L valley effective mass, $m*_\mathrm{L}$	$0.29m_0$	$0.42m_0$	$0.56m_0$
X valley effective mass, $m*_\mathrm{X}$	$0.64m_0$	$0.74m_0$	$0.85m_0$
Hole effective mass, m_0*	$0.5m_0$	$0.36m_0$	$0.5m_0$

it. We use semiconductor data as reported in [11, 19]. The absorption depth is dependent on the incident wavelength. We calculated it according to the data presented in [20], [21],[22], [23], intermediate values that did not appear in the references were interpolated linearly. Some other semiconductor parameters used in the simulation are shown in Table 1. All simulations assumed a temperature of 300 K.

The transient photoinjection and subsequent charge separation leads to the emission of terahertz radiation, which in the far-field is given by

$$E_{\mathrm{THz}}(t) = \frac{\partial J_z(t)}{\partial t}, \tag{1}$$

where J_z is the current density in the z direction. The current densities in the x and y directions have no contribution to the terahertz electric field given that they cancel out owing to symmetry. We perform sets of simulations for InAs, InGaAs and GaAs where the excitation photon energy varies starting from the corresponding Γ valley energy at a constant laser fluence of 382 nJ/cm^2. Normalized waveforms for all three sets of simulations are shown in Fig. 1.

The power emitted in each case was calculated by integrating the square of the electric field over the 5 ps period that the simulations lasted, and is given by

$$P_{\mathrm{THz}} = \int |E_{\mathrm{THz}}(t)|^2\, dt. \tag{2}$$

The emitted power as function of the pump photon energy is shown in Fig. 2. All three semiconductors show very pronounced increase in their emission with photon energy. Some features associated to the side valley transitions are also visible in the curves. The energy corresponding to 800 nm (1.54 eV) is indicated by a vertical dashed line. Many studies have compared the performance of these semiconductors at that wavelength, which is commonly used because of the availability of ultrafast Ti:sapphire lasers. A very significant power difference, exceeding one order of magnitude, is seen between GaAs and InAs. A quantitative comparison of the amplitudes at 800 nm is shown in the bar plot in Fig. 3b where InAs emits about 90 times the power emitted by GaAs. This difference in performance has been experimentally observed and power differences between ×44 and ×69 when comparing GaAs and InAs have been reported [3, 4]. This difference has historically been attributed to the larger contrast of diffusion of electrons and holes in InAs in comparison to GaAs, which is, at its time, associated to their contrast in mobilities. Yet, the contrast in mobilities does not have a significant dependence with the excess pump photon energy, then the increase in emitted power as a function of the pump photon energy can not be explained just by the difference in mobilities of the semiconductors.

Given that the curves presented in Fig. 2 were calculated for constant pump fluence, larger photon energies imply smaller numbers of photons per pump pulse, however, we can see that the emitted terahertz power in-

AIP Publishing

This manuscript was accepted by Appl. Phys. Lett. Click here to see the version of record.

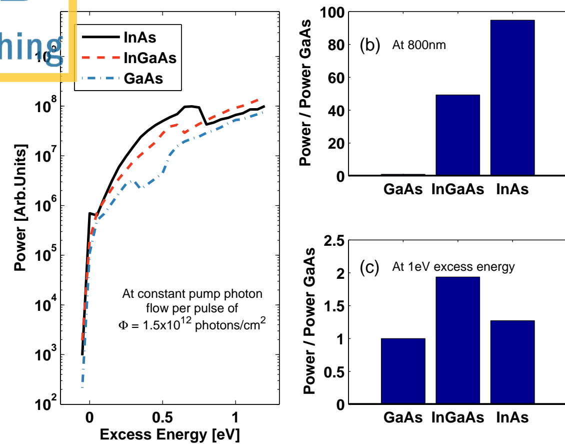

FIG. 3. (a) Emission power as function of excess energy from the Γ valley for each material. For these results, a constant pump photon flow per excitation pulse of 1.5×10^{12} photons/cm^2 was considered. (b) Ratio of emitted power to emitted power for GaAs for constant pump fluence at 800 nm (1.55 eV) excitation energy. (c) Ratio of emitted power to emitted power for GaAs at 1 eV of excess energy from Γ at constant pump photon flow per pulse.

creases with pump photon energy regardless of the fact that less electron-hole pairs are being excited.

In order to understand the previous observations we ran an additional set of simulations; this time the number of photons was constant for all wavelengths, this way the number of photo carriers is no longer a variable to be taken into account. The emitted terahertz power is shown in Fig. 3a. In this case the emitted power is shown as a function of pump photon's bangap excess energy, instead of their absolute energy. Firstly it is clear that now the differences in terahertz emission are significantly smaller, a comparison between all three semiconductors at 1 eV excess energy is shown in Fig. 3c, where they generate similar powers within a factor of 2. This means that the difference of mobilities between the three semiconductors only explains small differences, well below an order of magnitude of efficiency, when the semiconductors are pumped with the same number of photons and with the same bandgap excess energy. Yet, for constant photon flow, an even more pronounced dependance of the power emitted with excess energy is observed for all three semiconductors. From E_Γ to $E_\Gamma+1\,$eV there is an emitted power increase exceeding 1 order of magnitude. This suggests that the initial carrier energy is more important than the mobility difference, as has traditionally been considered.

From the observations in the previous paragraphs we can conclude that the initial kinetic energy of carriers is central to explain the extraordinary difference in emission between the three semiconductors at 800 nm. We also conclude that the difference in mobilities of the semiconductors accounts only for a relatively small part of their performance differences. Finally we can say that post-excitation ballistic motion is more relevant than diffusion in order to understand the carrier dynamics that leads to emission of terahertz from unbiased semiconductor surfaces and the relative importance of drift current in comparison to the ballistic motion depends on the comparison of the initial kinetic energy $h\nu - E_{\rm bangap}$ and the surface potential energy $eV_{\rm pin}$.

The authors would like to acknowledge the Universidad Autonoma de Aguascalientes (project grant PIM16-5) and Consejo Nacional de Ciencia y Tecnologia (grant numbers 255114 and 252939).

ACCEPTED MANUSCRIPT

[1] Y. Ko, S. Sengupta, S. Tomasulo, P. Dutta, and I. Wilke, Phys. Rev. B **78**, 035201 (2008).
[2] K. Liu, J. Xu, T. Yuan, and X. Zhang, Phys. Rev. B **73**, 155330 (2006).
[3] R. Adomavicius, A. Krotkusa, G. Molisa, A. Urbanowicza, and V. Malevich, Acta Physica Polonica A **113**, 859 (2008).
[4] J. L. Coutaz, V. L. Malevich, R. Adomaviius, and A. Krotkus, Comptes Rendus Physique **9**, 130 (2008).
[5] M. E. Barnes, D. McBryde, G. J. Daniell, G. Whitworth, A. L. Chung, A. H. Quarterman, K. G. Wilcox, A. Brewer, H. E. Beere, D. A. Ritchie, and V. Apostolopoulos, Optics Express **20**, 8898 (2012).
[6] A. Biinas, V. Paebutas, and A. Krotkus, Physica B: Condensed Matter **404**, 3386 (2009).
[7] E. A. P. Prieto, S. A. B. Vizcara, A. S. Somintac, A. A. Salvador, E. S. Estacio, C. T. Que, K. Yamamoto, and M. Tani, J. Opt. Soc. Am. B **31**, 291 (2014).
[8] J. Lloyd-Hughes, E. Castro-Camus, and M. B. Johnston, Solid State Commun. **136**, 595 (2005).
[9] J. N. Heyman, N. Coates, A. Reinhardt, and G. Strasser, Applied Physics Letters **83**, 5476 (2003).
[10] T. Hattori, S. Arai, and K. Tukamoto, Japanese Journal of Applied Physics **43**, 7546 (2004).
[11] M. B. Johnston, D. M. Whittaker, A. Corchia, A. G. Davies, and E. H. Linfield, Phys. Rev. B **65**, 165301 (2002).
[12] D. F. Liu and D. Xu, Appl. Opt. **46**, 789 (2007).
[13] V. Apostolopoulos and M. E. Barnes, Journal of Physics D: Applied Physics **47**, 374002 (2014).
[14] P. Gu, M. Tani, S. Kono, K. Sakai, and X.-C. Zhang, Journal of Applied Physics **91**, 5533 (2002).
[15] R. Mueckstein, O. Hatem, M. Natrella, J. R. Freeman, C. S. Graham, C. C. Renaud, A. J. Seeds, E. H. Linfield, A. G. Davies, P. J. Cannard, M. J. Robertson, D. G. Moodie, and O. Mitrofanov, in *2014 39th International Conference on Infrared, Millimeter, and Terahertz waves (IRMMW-THz)* (2014) pp. 1–2.
[16] R. Mueckstein, M. Natrella, O. Hatem, J. R. Freeman, C. S. Graham, C. C. Renaud, A. J. Seeds, E. H. Linfield,

This manuscript was accepted by Appl. Phys. Lett. Click here to see the version of record.

AIP Publishing

A. G. Davies, P. J. Cannard, M. J. Robertson, D. G. Moodie, and O. Mitrofanov, IEEE Transactions on Terahertz Science and Technology **5**, 260 (2015).

[17] S. C. Corzo-Garcia, A. I. Hernandez-Serrano, E. Castro-Camus, and O. Mitrofanov, Phys. Rev. B **94**, 045301 (2016).

[18] E. Castro-Camus, M. Johnston, and J. Lloyd-Hughes, Semiconductor Science and Technology **27**, 115011 (2012).

[19] NSM semiconductor archive. URL. http://www.ioffe.ru/SVA/NSM/Semicond/.

[20] J. R. Dixon and J. M. Ellis, Phys. Rev. **123**, 1560 (1961).

[21] D. E. Aspnes and A. A. Studna, Phys. Rev. B **27**, 985 (1983).

[22] H. C. C. Jr., D. D. Sell, and K. W. Wecht, Journal of Applied Physics **46**, 250 (1975), http://aip.scitation.org/doi/pdf/10.1063/1.321330.

[23] S. Adachi, "Optical properties," in *Physical Properties of III-V Semiconductor Compounds* (Wiley-VCH Verlag GmbH & Co. KGaA, 2005) pp. 135–192.

ACCEPTED MANUSCRIPT

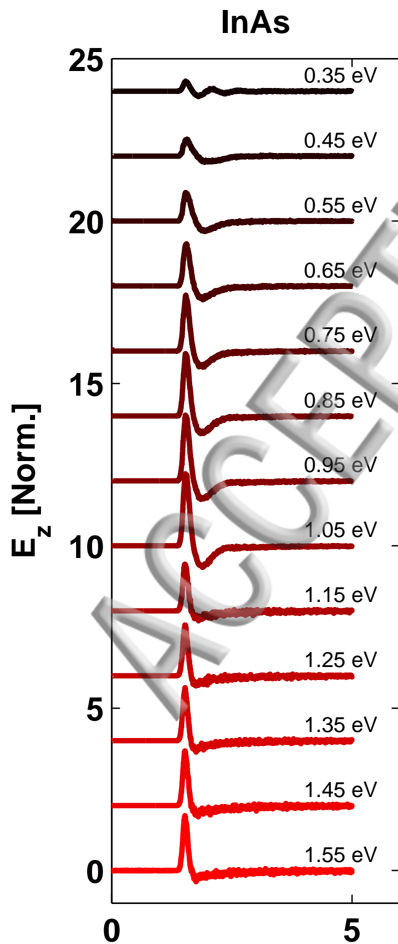
InAs
25
20
15
10
5
0
0
5
E_z [Norm.]
0.35 eV
0.45 eV
0.55 eV
0.65 eV
0.75 eV
0.85 eV
0.95 eV
1.05 eV
1.15 eV
1.25 eV
1.35 eV
1.45 eV
1.55 eV
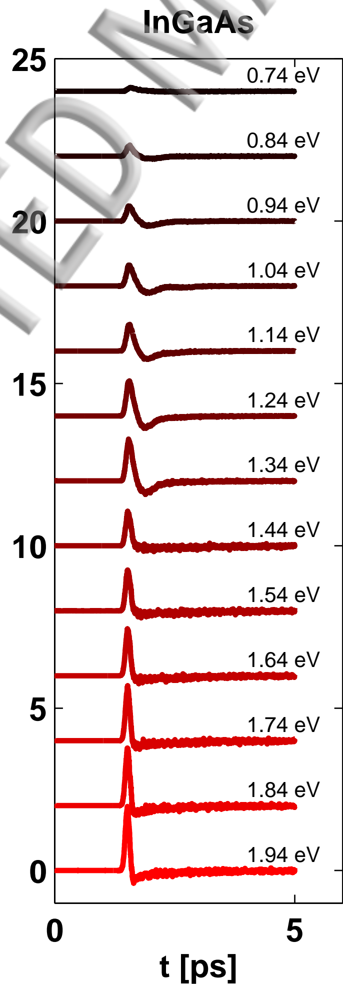
InGaAs
25
20
15
10
5
0
0
5
t [ps]
0.74 eV
0.84 eV
0.94 eV
1.04 eV
1.14 eV
1.24 eV
1.34 eV
1.44 eV
1.54 eV
1.64 eV
1.74 eV
1.84 eV
1.94 eV
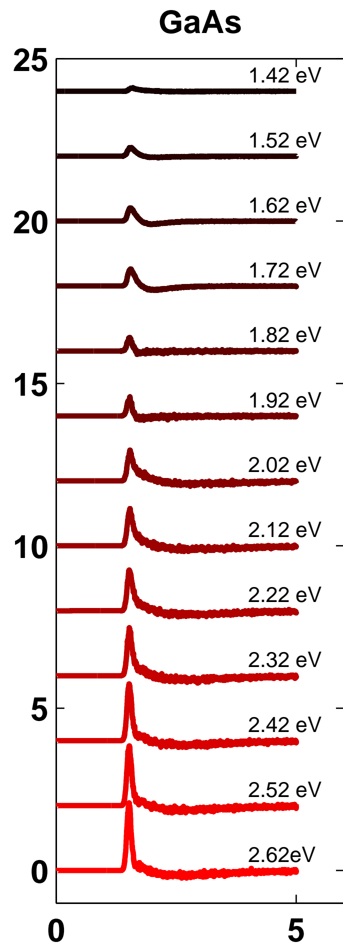
GaAs
25
20
15
10
5
0
0
5
1.42 eV
1.52 eV
1.62 eV
1.72 eV
1.82 eV
1.92 eV
2.02 eV
2.12 eV
2.22 eV
2.32 eV
2.42 eV
2.52 eV
2.62eV

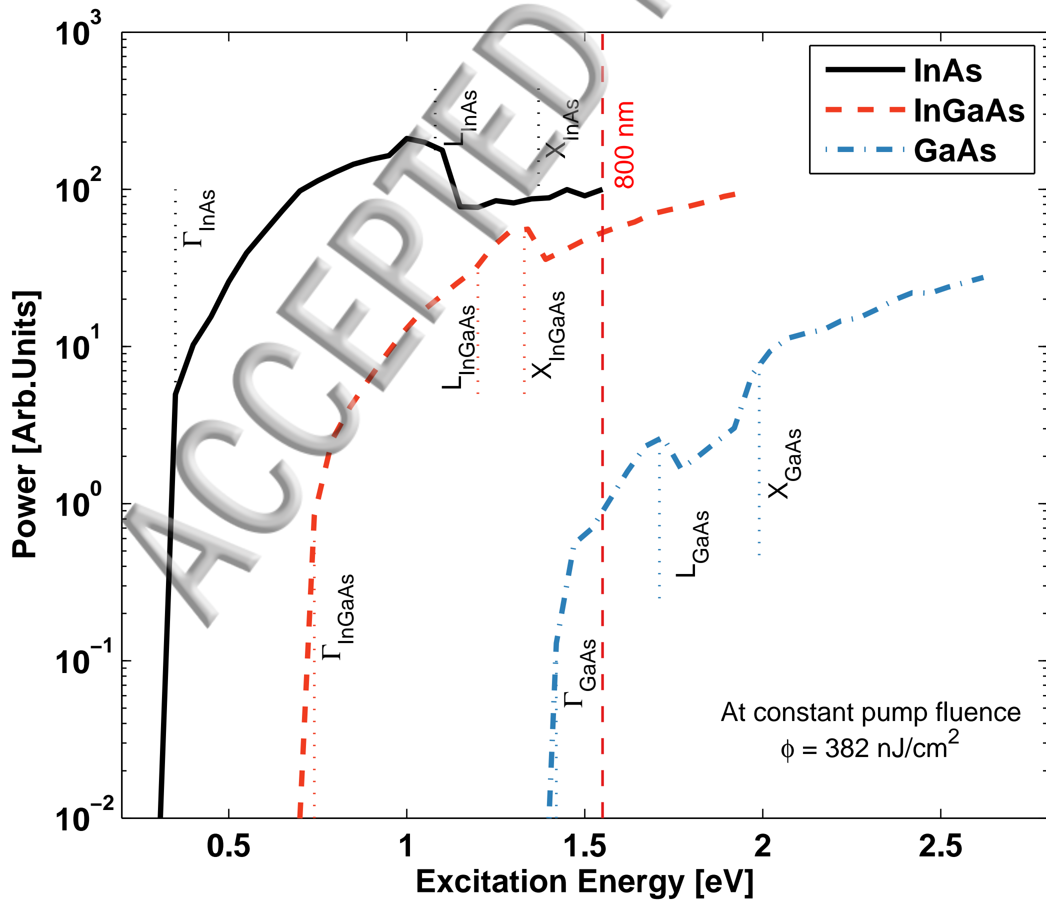

ACCEPTED M

InAs
InGaAs
GaAs
10^9
10^8
10^7
10^6
10^5
10^4
10^3
10^2
Power [Arb.Units]
0
0.5
1
Excess Energy [eV]
At constant pump photon flow per pulse of $\Phi = 1.5\mathrm{x}10^{12}$ photons/cm^2

ACCEPTED M